

Complete Active Space Iterative Coupled Cluster Theory

Robin Feldmann,[†] Max Mörchen,[†] Jakub Lang,[‡] Michał Lesiuk,[‡] and Markus
Reiher^{*,†}

[†]*ETH Zürich, Department of Chemistry and Applied Biosciences, Vladimir-Prelog-Weg 2,
8093 Zürich, Switzerland*

[‡]*Faculty of Chemistry, University of Warsaw
Pasteura 1, 02-093 Warsaw, Poland*

E-mail: mreiher@ethz.ch

Abstract

In this work, we investigate the possibility of improving multireference-driven coupled cluster (CC) approaches with an algorithm that iteratively combines complete active space (CAS) calculations with tailored CC and externally corrected CC. This is accomplished by establishing a feedback loop between the CC and CAS parts of a calculation through similarity transformation of the Hamiltonian with those CC amplitudes that are not encompassed by the active space. We denote this approach the complete active space iterative coupled cluster (CASiCC) ansatz. We investigate its efficiency and accuracy in the singles and doubles approximation by studying the prototypical molecules H_4 , H_8 , H_2O , and N_2 . Our results demonstrate that CASiCC systematically improves on the single-reference CCSD and the ecCCSD methods across entire potential energy curves, while retaining modest computational costs. However, the tailored coupled cluster method shows superior performance in the strong correlation

regime suggesting that its accuracy is based on error compensation. We find that the iterative version of externally corrected and tailored coupled cluster methods converge to the same results.

1 Introduction

A nagging issue in contemporary electronic structure theory is the notorious static-dynamic correlation problem. It will manifest itself if the Hartree–Fock (HF) determinant provides not just an inaccurate, but a qualitatively incorrect representation of the electronic structure. As a consequence, multiple determinants in a full configuration interaction (FCI) expansion of the electronic state possess similar nonnegligible configuration interaction (CI) coefficients. In such cases, approximate methods that construct excitations systematically from a single reference determinant, such as coupled cluster (CC) Møller–Plesset perturbation theory, CI with singles and doubles, yield either inaccurate or even completely unreliable results.^{1,2}

Then, multireference methods are required which rely on selecting a model space built from a subset of determinants that have significant weights in the FCI expansion. If the model space is constructed from all possible excitations from a set of occupied orbitals into a set of unoccupied (or virtual) orbitals, the approach will be referred to as a complete active space (CAS) method³ (cf. also the first-order reaction space approach⁴). The prevailing strategy for tackling multireference problems currently hinges on a self-consistent field (SCF) optimization of the orbitals and CI-coefficients of the CAS configuration interaction (CASCI) wave function, called the CASSCF method.⁵ Since exactly diagonalizing the Hamiltonian in the CAS approach scales factorially with the number of electrons and orbitals, approximate schemes were developed. Examples are perturbatively selected CI,^{6,7} heat-bath CI,^{8,9} the density matrix renormalization group (DMRG),^{10–22} FCI quantum Monte Carlo,^{23,24} and

* Corresponding author.

many-body expanded FCI.²⁵ For an overview of modern FCI methods and their comparison see Ref. 26.

Following the diagonalization of the Hamiltonian in the CAS approach, requires one to then consider those orbitals neglected from the CAS in the first place. Otherwise, dynamic correlation would be lacking and lead to inaccurate energies. Dynamic correlation is often accounted for using multireference perturbation theory (MRPT). There is some freedom in choosing the zeroth-order Hamiltonian²⁷ resulting in different flavors of MRPT as in CAS second-order²⁸ perturbation theory (CASPT2) or N -electron valence state second-order perturbation theory (NEVPT2).²⁹ However, MRPT comes with significant drawbacks: (i) perturbation theory cannot deliver high accuracy,^{30,31} (ii) the size of the CAS is constrained by the substantial computational demands associated with the evaluation of many-body reduced density matrices (RDMs), and (iii) because the size of the CAS is limited, it may not always be possible to include all important determinants in the CAS, which gives rise to the intruder state problem that results in considerable numerical instabilities.

One possibility to improve upon the accuracy of MRPT is the multireference CI (MRCI)^{32–42} approach, where the dynamic correlation is accounted for by diagonalizing the Hamiltonian in the basis of determinants generated from excitations from a multi-determinantal reference. However, its considerable computational demand (a consequence of the high-order RDMs required) restricts its applicability to small systems.

For single-reference systems, the coupled cluster (CC) method is the state of the art, especially in the form of the coupled cluster singles and doubles (CCSD) model with an additional non-iterative, perturbative triple component, known as CCSD(T).^{43,44} This has naturally led to the active development of multireference coupled cluster (MRCC) approaches.^{42,45–61} However, the transition from single reference CC (SRCC) to MRCC proved to be far from straightforward and a multitude of issues surfaced: (i) multiple-parentage problem that creates redundancies, (ii) intruder states, and (iii) non-terminating commutator expansions.^{42,60,61} These obstacles have not been overcome entirely, and consequently, no generally applicable

MRCC method has emerged yet.⁶⁰

Multireference-driven SRCC methods offer a practical alternative to the genuine MRCC methods. These methods, introduced by Oliphant and Adamowicz,⁶² Paldus and colleagues,^{63–67} and Stolarczyk,⁶⁸ account for multireference effects by keeping MRCI-derived cluster amplitudes fixed while optimizing the remaining amplitudes within the SRCC framework. The fixed amplitudes, known as internal amplitudes, are associated with excitations within the model (or internal) space, typically the CAS. The amplitudes related to excitations within the external space—comprised of all other orbitals—are denoted external amplitudes. A particularly practical variant of the multireference-driven methods is the tailored CC (TCC) method, introduced by Kinoshita, Hino, and Bartlett.⁶⁹ Computationally less appealing, but well explored is the externally correct CCSD (ecCCSD) method.^{70–74} However, a severe limitation of multireference-driven methods is the choice of the reference determinant. This limitation makes CCSD more accurate than TCCSD within the single-reference regime due to the absence of back-coupling between the external and internal amplitudes and reduces the accuracy in the multireference regime due to the bias of the reference determinant.^{75–77}

While CC theory is often seen as a non-linear wave function formulation, it can also be viewed as an effective Hamiltonian theory.⁷⁸ This interpretation establishes a connection between CC and the similarity renormalization group (SRG) approach, which was developed by Głazek and Wilson⁷⁹ and by Wegner.⁸⁰ The SRG method relies on a flow equation for the unitary transformation of the Hamiltonian. This equation is integrated with a suitably chosen generator for the transformation, such that the off-diagonal elements of the Hamiltonian are vanishing. This idea was later applied in chemistry by White⁸¹ who extended the SRG method to transformations in the many-body space. This flavor of the SRG has also found numerous applications in nuclear structure theory where it is usually denoted as the in-medium SRG (IMSRG).^{82–84} The IMSRG is a relatively new method that has seen rapid development in recent years.^{85–87}

Based on the idea of the IMSRG and White’s canonical transformation, Evangelista

developed the driven SRG (DSRG) method and applied it to chemical problems.^{88,89} The advantage of the DSRG is that it does not require the integration of the flow equation, instead it can be solved in one step. Later, the DSRG was also generalized to a multireference method⁹⁰ based on the Mukherjee–Kutzelnigg normal ordering.^{48,49} Moreover, based on the DSRG, Li and Evangelista developed a new MRPT which alleviates the intruder state problem.^{90,91} However, a notable drawback of the DSRG method is its dependency on the flow parameter. The choice of this parameter significantly affects the energy and, if applied within the MRPT formulation, it also affects the intruder state problem.⁹⁰

In this work, we build upon the TCCSD and the ecCCSD methods, the SRG approach, and also on recent advances in SRCC theory, namely the subalgebra formulation of CC.^{92–95} Our approach starts from a standard CASCI plus TCCSD (or ecCCSD) calculation. We investigate the possibility of iteratively improving the TCCSD or ecCCSD wave function by applying a similarity transformation of the Hamiltonian with the CC amplitudes from the external space. The many-body expansion of the similarity-transformed Hamiltonian is then truncated after a given order. This results in a nonhermitian Hamiltonian that is subsequently projected into the CAS many-body space and then diagonalized with a nonhermitian FCI solver. Building on the work of Kowalski, who demonstrated that an iterative solution of the CC equations in two separate subalgebras is equivalent to solving the CC equations in the entire space,⁹² we reapply the TCCSD (or ecCCSD) approach. The Hamiltonian is then subjected to another transformation and once again diagonalized. This process is iteratively repeated until convergence is attained. Our reasoning is the following: with this strategy we aim to address the challenge of the multireference-driven CC methods, where issues arise due to a lack of feedback between the amplitudes associated with the CAS and the external space. We note that Li and Evangelista have developed an iterative method based on the DSRG^{96,97} and similar ideas for the CC method have been proposed in the literature before,^{60,98,99} but have not been studied in actual calculations.

This work is organized as follows: in Sec. 2 we provide the derivation of the working

equations of the complete active space with iterative coupled cluster and we present a detailed explanation of the algorithm and its implementation. In Sec. 3 we describe our computational methodology and we continue in Sec. 4 by presenting the computational results for several small molecules, namely H₄, H₈, H₂O, and N₂.

2 Theory

2.1 The coupled cluster ansatz and its excitation subalgebras

In this section, we briefly review the single reference coupled cluster ansatz and introduce the excitation subalgebras by Kowalski⁹² to define the CC equations in the internal space, which will correspond to the CAS, and the external space, which consists of all other excitations that are not contained in the CAS. This framework enables us to derive our iterative optimization algorithm, where the internal equations can be solved with any non-hermitian CASCI method, and the amplitudes extracted from the CASCI wave function are either inserted in the TCC or in the ecCC ansatz.

We introduce the nonrelativistic normal-ordered electronic Born–Oppenheimer Hamiltonian in second quantization

$$H = E_0 + \sum_{pq} F_{pq} \{p^\dagger q\} + \frac{1}{4} \sum_{pqrs} \langle pq || rs \rangle \{p^\dagger q^\dagger sr\}, \quad (1)$$

where F_{pq} is the Fock matrix and $\langle pq || rs \rangle$ are the antisymmetrized two-electron integrals. The latter are given in the physics notation. In this work, we follow the standard convention where p, q, r, s correspond to arbitrary orbitals, i, j, k, l, \dots to occupied orbitals, and a, b, c, d, \dots to unoccupied ones, while curly brackets refer to a normal-ordered string of second quantization operators. The full coupled cluster (FCC) wave function ansatz is an exact ansatz to solve

the time-independent electronic Schrödinger equation and can be written as

$$|\Psi_{\text{FCC}}\rangle = e^T |0\rangle, \quad (2)$$

where $|0\rangle$ is the reference determinant and T is the cluster operator defined as

$$T = \sum_n^N T_n. \quad (3)$$

Here, N is the number of electrons in the system and T_n contains n -body excitations and reads

$$T_n = \frac{1}{(n!)^2} \sum_{\substack{i_1 \dots i_n \\ a_1 \dots a_n}} t_{i_1 \dots i_n}^{a_1 \dots a_n} \{a_1^\dagger \dots a_n^\dagger i_n \dots i_1\}, \quad (4)$$

where, $t_{i_1 \dots i_n}^{a_1 \dots a_n}$, are the CC amplitudes which we aim to optimize. Equivalently, the FCI wave function,

$$|\Psi_{\text{FCI}}\rangle = (1 + C)|0\rangle, \quad (5)$$

also solves the Schrödinger equation exactly with the CI operator

$$C = \sum_n^N C_n, \quad (6)$$

and the n -body CI excitation operators

$$C_n = \frac{1}{(n!)^2} \sum_{\substack{i_1 \dots i_n \\ a_1 \dots a_n}} c_{i_1 \dots i_n}^{a_1 \dots a_n} \{a_1^\dagger \dots a_n^\dagger i_n \dots i_1\}. \quad (7)$$

By cluster analysis,¹⁰⁰ a mapping between the CI coefficients, $c_{i_1 \dots i_n}^{a_1 \dots a_n}$, and the CC amplitudes, $t_{i_1 \dots i_n}^{a_1 \dots a_n}$, can be found. The associated determinant for a given string of second quantization operators acting on the reference is abbreviated as

$$|_{i_1 \dots i_n}^{a_1 \dots a_n}\rangle = \{a_1^\dagger \dots a_n^\dagger i_n \dots i_1\}|0\rangle. \quad (8)$$

To formulate the equation for the CC amplitude optimization in a convenient way, we introduce projection operators. The projector onto the reference determinant states

$$P = |0\rangle \langle 0|, \quad (9)$$

and the projector onto all excited determinants is given by

$$Q = \sum_n^N \sum_{\substack{i_1 < \dots < i_n \\ a_1 < \dots < a_n}} |_{i_1 \dots i_n}^{a_1 \dots a_n} \rangle \langle_{i_1 \dots i_n}^{a_1 \dots a_n} |. \quad (10)$$

Following Li and Paldus¹⁰¹ and Kowalski,⁹² the energy-independent CC equations for the amplitudes are written as

$$Q e^{-T} H e^T |0\rangle = Q (H e^T)_C |0\rangle = 0, \quad (11)$$

where the subscript C means that only the connected diagrams are to be considered. By solving Eq. (11), the CC amplitudes, $t_{i_1 \dots i_n}^{a_1 \dots a_n}$, can be obtained, and the energy can be evaluated according to

$$E = \langle 0 | (H e^T)_C |0\rangle. \quad (12)$$

Next, we divide the space of excitations into the internal excitations which denote the excitations associated with distributing K electrons among L orbitals often denoted as $\text{CAS}(K,L)$, and into the external space, which contains all other determinants. We introduce the internal cluster operator T^{int} , which generates the CASCI wave function in this space as

$$|\Psi_{\text{int}}\rangle = e^{T^{\text{int}}} |0\rangle. \quad (13)$$

Additionally, we introduce the external cluster operator, T^{ext} , which generates all other

excitations. The FCC wave function can then be expressed as

$$|\Psi_{\text{FCC}}\rangle = e^{T^{\text{ext}}+T^{\text{int}}} |0\rangle = e^{T^{\text{ext}}} |\Psi_{\text{int}}\rangle. \quad (14)$$

The external and internal spaces can be viewed as the subalgebras introduced by Kowalski⁹² which enables us to rewrite the CC equations in a form that is suitable for our purpose. We rewrite the projection operator onto the excited-determinant manifold of Eq. (10) as

$$Q = Q^{\text{int}} + Q^{\text{ext}}, \quad (15)$$

where Q^{int} projects onto all excited determinants from the CAS(K, L), and Q^{ext} projects onto the external determinants. Consequently, we can divide the Schrödinger equation into an internal part

$$(P + Q^{\text{int}})H e^{T^{\text{ext}}} |\Psi_{\text{int}}\rangle = E(P + Q^{\text{int}}) e^{T^{\text{ext}}} |\Psi_{\text{int}}\rangle, \quad (16)$$

and an external one

$$Q^{\text{ext}}H e^{T^{\text{ext}}+T^{\text{int}}} |0\rangle = EQ^{\text{ext}} e^{T^{\text{ext}}+T^{\text{int}}} |0\rangle. \quad (17)$$

We introduce the similarity-transformed Hamiltonian

$$\bar{H}^{\text{ext}} = e^{-T^{\text{ext}}} H e^{T^{\text{ext}}}, \quad (18)$$

and insert the identity $e^{T^{\text{ext}}} e^{-T^{\text{ext}}}$ in front of the Hamiltonian in Eq. (16), such that we obtain

$$(P + Q^{\text{int}}) e^{T^{\text{ext}}} \bar{H}^{\text{ext}} |\Psi_{\text{int}}\rangle = E(P + Q^{\text{int}}) e^{T^{\text{ext}}} |\Psi_{\text{int}}\rangle. \quad (19)$$

Kowalski has demonstrated in Ref. 92 that $e^{T^{\text{ext}}}$ does neither contribute to the left nor to the right hand side of Eq. (19), and hence, the equation can be simplified as

$$(P + Q^{\text{int}}) \bar{H}^{\text{ext}} |\Psi_{\text{int}}\rangle = E(P + Q^{\text{int}}) |\Psi_{\text{int}}\rangle. \quad (20)$$

In this form, it becomes apparent that the amplitudes T^{int} can be obtained by solving the nonhermitian eigenvalue problem of Eq. (20), which means that we diagonalize the similarity-transformed Hamiltonian, \bar{H}^{ext} , in the internal space. The external amplitudes, however, can be obtained by solving the external Schrödinger equation, Eq. (17), with the conventional coupled cluster algorithm, while keeping the internal amplitudes fixed. This, of course, corresponds to the TCC model. The new idea in this work is to iteratively solve Eqs. (20) and (17) in an alternating way until self-consistency is reached. However, solving the equations exactly would not yield any computational advantage. In the next section, we therefore discuss approximations to make this idea practical. We also describe the ecCC method, which can replace TCC as an alternative ansatz.

2.2 Configuration interaction with iterative coupled cluster

In this section, we discuss approximations to solve Eqs. (20) and (17). First, we always limit the excitation degree in the external space to singles and doubles in this work. That is, we rely on TCCSD to solve the external equations

$$T_{\text{SD}}^{\text{ext}} = T_1^{\text{ext}} + T_2^{\text{ext}}, \quad (21)$$

which leads to the singles and doubles similarity-transformed Hamiltonian

$$\bar{H}_{\text{SD}}^{\text{ext}} = e^{-T_{\text{SD}}^{\text{ext}}} H e^{T_{\text{SD}}^{\text{ext}}}. \quad (22)$$

The exact similarity transformation of Eq. (22) yields up to six-body interactions, which would require storing up to twelve-index tensors. This is prohibitive in practice even for the smallest systems. The cheapest reasonable truncation scheme appears to be the Baker–Campbell–Hausdorff (BCH) expansion of the similarity-transformed Hamiltonian truncated

after the second order to obtain

$$\bar{H}_{\text{SD}}^{\text{ext},(2)} = \chi_0 + \sum_{pq} \chi_{pq} \{p^\dagger q\} + \frac{1}{4} \sum_{pqrs} \chi_{pqrs} \{p^\dagger q^\dagger sr\}. \quad (23)$$

The equations for obtaining the matrix elements χ_0 , χ_{pq} , and χ_{pqrs} can be obtained with standard textbook methods² or, in our case, automatic equation generation tools.¹⁰² To improve upon this, we can truncate the expansion after the third order

$$\bar{H}_{\text{SD}}^{\text{ext},(3)} = \bar{H}_{\text{SD}}^{\text{ext},(2)} + \frac{1}{(3!)^2} \sum_{pqrst} \chi_{pqrst} \{p^\dagger q^\dagger r^\dagger uts\}, \quad (24)$$

or after the fourth order

$$\bar{H}_{\text{SD}}^{\text{ext},(4)} = \bar{H}_{\text{SD}}^{\text{ext},(3)} + \frac{1}{(4!)^2} \sum_{pqrstuvw} \chi_{pqrstuvw} \{p^\dagger q^\dagger r^\dagger s^\dagger vwut\}. \quad (25)$$

The three- and four-body matrix elements are given in physics notation and are fully antisymmetrized. However, evaluating them in the entire space would already be prohibitive for medium-sized systems, since the Hamiltonian is projected into the internal space, only the entries of the tensors in the active space have to be computed and stored. For comparison, the memory scaling of the truncation after the third order is that of CASPT2, where the three-body reduced density matrix is required, and the memory scaling of the truncation after the fourth order is that of NEVPT2, where four-body reduced density matrix elements are needed.

We note that, if the BCH expansion is truncated, the transformation is no longer of the type of a similarity transformation. Consequently, the eigenvalues of the transformed Hamiltonian will not exactly match those of the original Hamiltonian.

The truncation of the BCH expansion also results in a dependency on the definition of the vacuum state. E.g., a truncated Hamiltonian ordered with respect to the physical vacuum may have a different spectrum than a normal-ordered Hamiltonian with respect

to the Fermi vacuum. However, by including higher-body operators, this discrepancy will become negligible.

In practice, we solve the following eigenvalue problem in the internal space

$$(P + Q^{\text{int}})\bar{H}_{\text{SD}}^{\text{ext},(n)}|\Psi_{\text{int}}\rangle = E_{\text{SD}}^{(n)}(P + Q^{\text{int}})|\Psi_{\text{int}}\rangle, \quad n \in \{2, 3, 4\}. \quad (26)$$

Due to the structure of the CC equations, the similarity transformation is not truncated in the equations for the external amplitudes. We extract the singles and doubles amplitudes from the internal wave function in TCCSD,

$$T_{\text{TCCSD}}^{\text{int}} = T_1^{\text{int}} + T_2^{\text{int}}, \quad (27)$$

and the triples and quadruples in ecCCSD,

$$T_{\text{ecCCSD}}^{\text{int}} = T_3^{\text{int}} + T_4^{\text{int}}. \quad (28)$$

In the TCCSD case, the external equations read

$$Q_{\text{SD}}^{\text{ext}}(H e^{T_{\text{SD}}^{\text{ext}}+T_{\text{TCCSD}}^{\text{int}}})_C |0\rangle = 0, \quad (29)$$

whereas for ecCCSD, the internal and external singles and doubles are optimized in the presence of the internal triples and quadruples

$$(Q_{\text{SD}}^{\text{int}} + Q_{\text{SD}}^{\text{ext}})(H e^{T_{\text{SD}}^{\text{ext}}+T_{\text{SD}}^{\text{int}}+T_{\text{ecCCSD}}^{\text{int}}})_C |0\rangle = 0. \quad (30)$$

The key ideas of our approach are therefore: (i) the amplitudes are optimized in the presence of dynamic correlation encoded by the external amplitudes entering Eq. (26), and (ii) the external amplitudes are affected by static correlations encoded in the internal amplitudes entering Eqs. (29) and (30). The final wave function is an improved CCSD wave function,

written as

$$|\Psi_{\text{CASiCCSD}(n)}\rangle = e^{T_{\text{SD}}^{\text{int}} + T_{\text{SD}}^{\text{ext}}} |0\rangle. \quad (31)$$

Here, we introduced the acronym CASiCCSD(n) standing for complete active space iterative CCSD. Depending on the MR-driven CC method, we refer to the approach as CASiecCCSD(n) or CASiTCCSD(n), where n denotes the order after which the BCH expansion is truncated. More generally, we denote the method as CASiCC.

To conclude this section, we summarize the CASiCC algorithm at the example of the CASiTCCSD(3) model in Fig. 1: first, we start with a Hartree–Fock calculation to generate the initial hermitian Hamiltonian. This corresponds to the similarity-transformed $\bar{H}_{\text{SD}}^{\text{ext},(3)}$ with $T_{\text{SD}}^{\text{ext}} = 0$. Then, the Hamiltonian is diagonalized within the active space which gives an initial set of CASCI coefficients. With the singles and doubles CI-coefficients, we generate the initial internal amplitudes $T_{\text{SD}}^{\text{int}}$. Subsequently, we perform a TCCSD calculation to obtain the external amplitudes $T_{\text{SD}}^{\text{ext}}$. Up to this point, the algorithm corresponds to the TCCSD method. Next, we generate the first non-hermitian Hamiltonian, $\bar{H}_{\text{SD}}^{\text{ext},(3)}$, with the external amplitudes $T_{\text{SD}}^{\text{ext}}$. This Hamiltonian is then diagonalized to obtain a new set of CI coefficients, which are employed to generate the new internal amplitudes, $T_{\text{SD}}^{\text{int}}$ subjected to the TCCSD algorithm to generate a new set of external amplitudes, $T_{\text{SD}}^{\text{ext}}$. At this point, we check the energy difference between the current and the previous iteration. If the energy is converged, the algorithm is terminated, otherwise, $\bar{H}_{\text{SD}}^{\text{ext},(3)}$ is calculated with the new external amplitudes $T_{\text{SD}}^{\text{ext}}$ and the next iteration step begins.

3 Computational details

For nonhermitian n -body CASCI calculations, we have developed a Python program which exploits C++ routines with pybind11¹⁰³ for the performance sensitive tasks. This program can diagonalize real symmetric and nonsymmetric Hamiltonians with up to four-body operators and integrates the CC routines. We relied on Wick&d¹⁰² for the automatic code generation

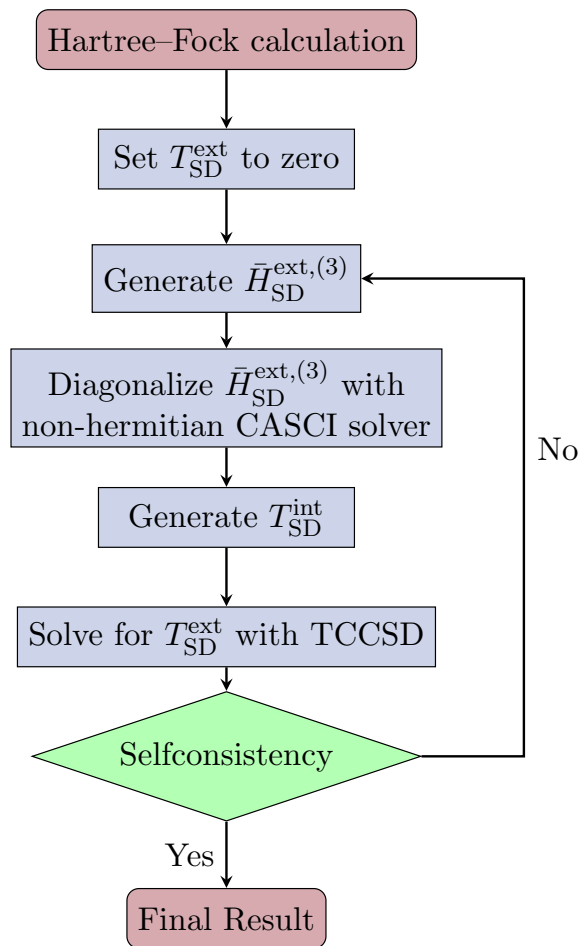


Figure 1: Flowchart for the CASiTCCSD(3) algorithm.

for the CC equations, for the similarity transformation, and for the transformation of the CI coefficients to CC amplitudes. The source code of our program and all data presented in this work have been published on Zenodo.¹⁰⁴

All DMRG calculations were conducted with the QCMAQUIS software package.¹⁰⁵ We sorted the orbitals on the lattice according to the Fiedler ordering^{106,107} and converged the energy up to 10^{-6} Hartree with a maximum bond dimension of 2000. We sorted the orbitals on the lattice according to the Fiedler ordering^{106,107} and converged the energy up to 10^{-6} Hartree with a maximum bond dimension, denoted by m , of 2000. It was shown before¹⁰⁸ that DMRG results obtained with a bond dimension of 2000 are converged up to 0.5 mHartree for N_2 with the cc-pVDZ basis set. Since N_2 is the largest system that we consider here, that bond dimension will be sufficient all other systems analyzed in this work. Furthermore, the accuracy of 0.5 mHartree meets our requirements for evaluating the performance of the CC methods.

The error of an electronic structure model ('M') at some point x on the potential energy curve measured against a reference model ('ref') is evaluated as $\Delta E(x) = E_M(x) - E_{\text{ref}}(x)$.

For the atomic orbital basis, we chose Pople¹⁰⁹ (for such small basis sets one can still obtain the FCI solution by direct diagonalization) and correlation consistent basis sets.¹¹⁰ The calculation of the molecular orbital integrals in the Hartree–Fock basis was performed with the PySCF program.^{111,112}

4 Results

4.1 H_4 and H_8 test systems

To demonstrate the effectiveness of the CASiCC method, we first examine the dissociation of the stretched H_4 system into two H_2 for a CAS(4,4). The geometric configuration of this system is illustrated in Fig. 2. In our comparative analysis of different methods, we specifically selected the stretched geometry with $k = 2 \text{ \AA}$ over the more commonly used $k = 1 \text{ \AA}$. This

decision was based on the observation that the former geometry yielded more pronounced differences between the methods, thereby providing a better basis for the comparative analysis. A key feature of this system is the adjustability of its multireference characteristics through the dissociation parameter α . Specifically, at $\alpha = 2 \text{ \AA}$, the ground state exhibits perfect degeneracy while for larger or smaller α values, dynamic correlation is dominating. To analyze the capabilities of our approach, we present a comparative analysis of the absolute error in electronic energies measured against the FCI energy along the dissociation curve. This comparison comprises CCSD, TCCSD, and ecCCSD, alongside our CASiTCCSD(n) and CASiecCCSD(n) models.

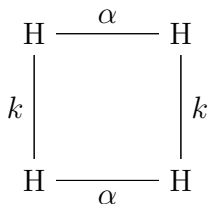


Figure 2: Geometry of the stretched H_4 system. The k parameter is fixed to 2 \AA and the α parameter is varied between 0.5 and 4 \AA .

Fig. 3 presents the absolute values of the errors of various single-reference and multireference-driven CC methods with respect to FCI. It is important to note that our choice of presenting absolute errors (rather than signed errors defined in the computational methodology section) because of the logarithmic scale leads to discontinuities in the curves shown. These arise when the potential energy curve of a method intersects with the FCI curve. Hence, the discontinuities in the curves of the absolute errors do not reflect actual discontinuities in the potential energy curves.

The first row of diagrams in Fig. 3 shows the errors of the CCSD, TCCSD, and ecCCSD energies. CCSD fails as α tends to 2 \AA from the left and right. The error approaches 10 mHartree at 2 \AA and is two to four orders of magnitude larger than in the dynamic correlation regime with $\alpha < 1 \text{ \AA}$ and $\alpha > 3 \text{ \AA}$. TCCSD also shows a large systematic error reaching more than 1 mHartree for $\alpha > 1 \text{ \AA}$. By contrast to CCSD, TCCSD features no spike

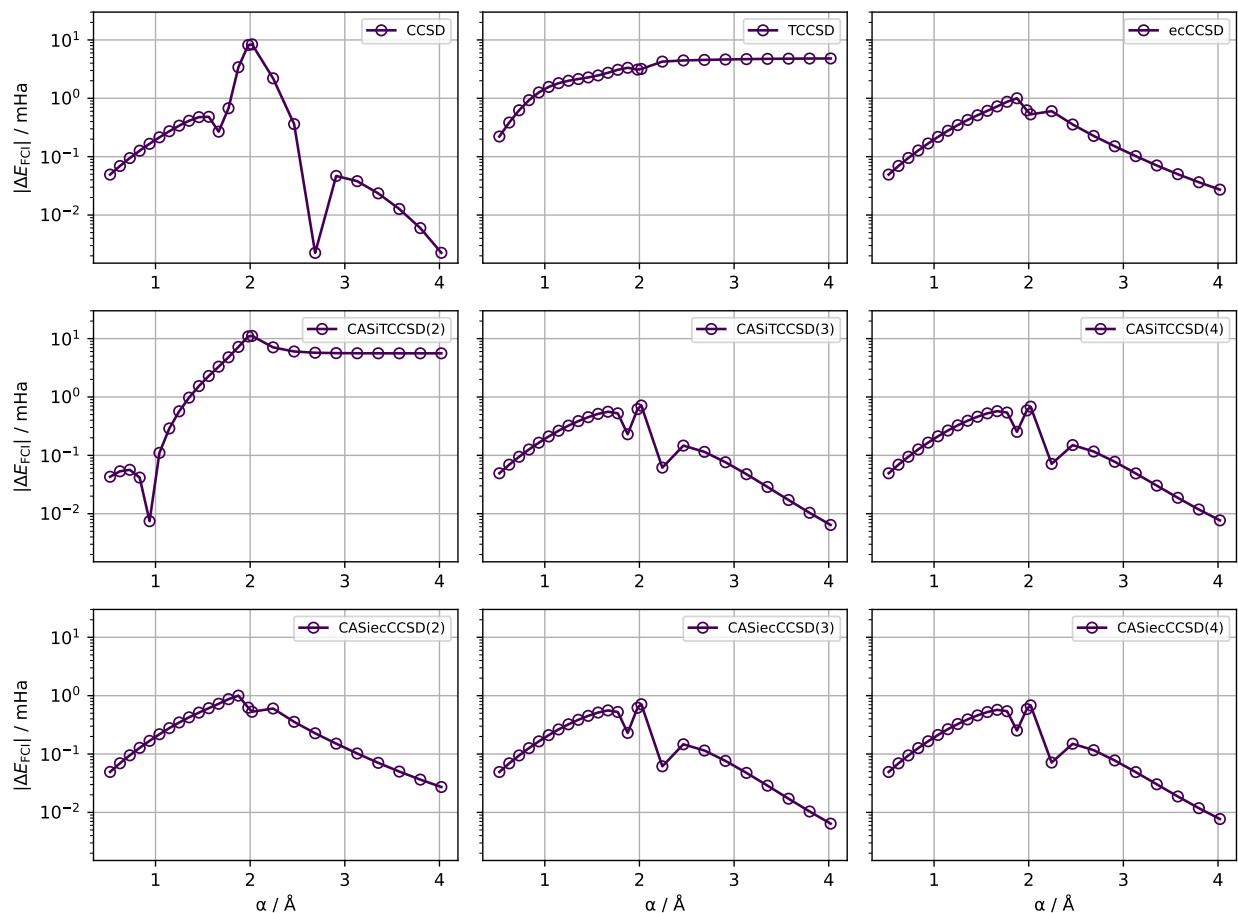


Figure 3: Absolute error of the electronic energy in mHartree with respect to FCI for the dissociation of H_4 in the geometry depicted in Fig. 2. Shown are results for CCSD, TCCSD, ecCCSD (top) and for different truncation schemes of the BCH expansion for CASiTCCSD (middle) and CASieccCSD (bottom). The cc-pVDZ basis set chosen yields 20 orbitals in total. The FCI calculations took all orbitals into account and we employed a CAS(4,4) for the multireference-driven CC methods.

at 2 Å and the error stays constantly high during dissociation. ecCCSD performs better than CCSD and TCCSD, but also shows a small spike at 2 Å where the error is above 1 mHartree.

The second row of Fig. 3 depicts the error of CASiTCCSD(n) with truncation orders $n = 2, 3, 4$ from left to right. For CASiTCCSD(2), the Hamiltonian expansion has not reached convergence at the second order. This is evident as there is a significant change in the energy error curve when transitioning from $n = 2$ to $n = 3$. However, the curves for $n = 3$ and $n = 4$ are virtually indistinguishable, suggesting convergence with respect to n has been reached for $n = 3$.

The third row of Fig. 3 shows the different truncation schemes for CASieCCSD(n). The CASieCCSD(2) results are similar to the ecCCSD results, with a slight improvement at $\alpha = 2$ Å. However, the absolute error is significantly different for $n > 2$, and similar to CASiTCCSD, it converged for $n = 3$ (when compared to $n = 4$). Intriguingly, for both, CASiTCCSD and CASieCCSD, the results are identical if $n > 2$. This indicates that our approach of accounting for static correlation, independently of whether through the inclusion of singles and doubles or through the inclusion of triples and quadruples from the CAS, does not affect the energy when applied in a self-consistent manner.

From a computational point of view, TCCSD is significantly more appealing. Specifically, ecCCSD necessitates the calculation of T_3 and T_4 amplitudes, which entail memory scalings of $\mathcal{O}(O^3V^3)$ and $\mathcal{O}(O^4V^4)$, respectively, where O and V represent the numbers of occupied and virtual orbitals within the active space, respectively. Moreover, the key challenges in the implementation of the (parent) ecCCSD are: (i) the transformation of CI coefficients to CC amplitudes is an issue when efficiency is a priority, and (ii) efficiently integrating the contributions of triples and quadruples into the singles and doubles residuals is equally challenging.

Given these considerations, the convergence of both, CASiTCCSD and CASieCCSD, to identical results favors the CASiTCCSD model in routine applications for feasibility reasons. CASiTCCSD circumvents the aforementioned computational complexities, making it a more

efficient and practical choice.

Table 1: Non-parallelity error (NPE) in mHartree with respect to FCI for the dissociation of the H_4 and H_8 systems with the geometries depicted in Figs. 2 and 4, respectively. For H_4 , we chose the cc-pVDZ basis set and a CAS(4,4) for the multireference-driven CC methods, whereas for H_8 , we chose the 6-31G basis set and a CAS(8,8).

	CCSD	TCCSD	ecCCSD
H_4	8.41	4.59	0.97
H_8	9.05	2.17	5.77
	CASiTCCSD(2)	CASiTCCSD(3)	CASiTCCSD(4)
H_4	11.12	0.71	0.68
H_8	6.00	6.82	6.83
	CASieCCSD(2)	CASieCCSD(3)	CASieCCSD(4)
H_4	0.97	0.71	0.68
H_8	6.76	6.82	6.83

Next, we focus on assessing the accuracy of the CASiCC models. Fig. 3 shows that, with the exception of CASiTCCSD(2), the CASiCC methods pose a systematic improvement over the CCSD method in the single and also multireference regime and they overall show the lowest error, also compared to TCCSD and ecCCSD. The non-parallelity errors (NPEs), that is the difference between the maximum and minimum error of the potential energy curves, are given in Table 1. According to the table, the accuracy of the models is increases according to: CCSD, TCCSD, ecCCSD followed by CASiTCCSD (except for $n = 2$) and CASieCCSD which have the same errors. Our findings also highlight a limitation of the standard TCCSD method, revealing that it does not consistently offer an improvement over the CCSD method.

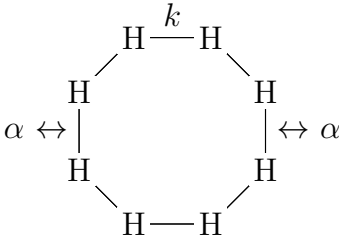


Figure 4: Geometry of the H_8 system. The k parameter denotes the bond distances for the H_2 units (left, right, upper and lower ones) which are fixed to 1 Å. The α parameters refers to shifting the left and right H_2 units and is varied between -0.22 and 0.22 Å, where $\alpha = 0$ corresponds to the octagon.

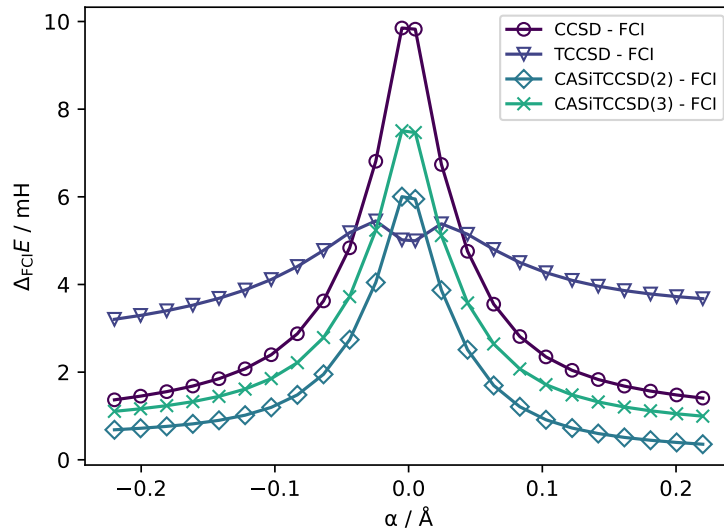


Figure 5: Error of the total electronic energy in Hartree with respect to FCI for the dissociation of the H_8 system in the geometry depicted in Fig. 4. Shown are results for TCCSD and for CASiTCCSD for different truncation schemes of the BCH expansion. We chose the small 6-31G basis set for the calculation which yields 16 orbitals, for which FCI results, taking all orbitals into account, can be obtained as reference. For the CASiCC calculations we employed a CAS(8,8).

Continuing our analysis, we turn to the octagonal H_8 model system, as illustrated in Fig. 4 with a CAS(8,8). As for the H_4 system, the multiconfigurational character of H_8 is adjustable through the parameter α . Our results reveal that, in accordance with our findings for H_4 , the CASiCC models exhibit convergence at truncation order $n = 3$ for H_8 . Moreover both CASiTCCSD and CASiecCCSD again yield identical results upon convergence, as shown in Tab. 1.

Fig. 5 presents the errors in total electronic energy (compared to FCI results) for various models: CCSD, TCCSD, CASiTCCSD(2), and CASiTCCSD(3). Similar to the trends observed for H_4 , CCSD performs well in the single-reference regime, but exhibits a pronounced peak in error at the point of degeneracy, $\alpha = 2$. TCCSD also shows again a rather constant relatively large error along the entire curve, but displays only a minor peak at $\alpha = 2$. CASiTCCSD again demonstrates systematic improvement over CCSD, yet the error at $\alpha = 2$ is larger than that of TCCSD. The error of CASiTCCSD(2) consistently remains lower than that of CASiTCCSD(3), possibly due to fortuitous error cancellation.

The NPEs of these methods are listed in Table 1. Here, CCSD shows the highest NPE, followed by the CASiCC methods and ecCCSD, while TCCSD exhibits the lowest NPE. Also from these results, it is evident that the CASiCC methods provide a systematic improvement over CCSD. However, TCCSD and ecCCSD might offer better performance, potentially due to error cancellation.

4.2 Potential energy curves of small molecules

For the small molecules studied in this section, we note that the iterative algorithm is usually converged to 10^{-10} Hartree in 5 to 15 macroiteration steps. Regarding the CC optimization of the external amplitudes, we employed the amplitudes from the previous iteration as a starting guess, which significantly accelerated convergence. The CC equations are usually converged in 2 to 3 iterations after the first few macro iterations.

4.2.1 Dissociation of N_2

To describe the bond-breaking in N_2 , we chose a CAS(6,6). The cc-pVDZ basis set yielded a total of 28 orbitals. Potential energy curves for CCSD, CASiTCCSD(2), CASiTCCSD(3), TCCSD, and DMRG (top figure), along with the deviation of the coupled cluster (CC) models compared to DMRG (bottom figure), are shown in Fig. 6.

As expected, CCSD completely fails in the dissociation limit, whereas TCCSD reliably describes the dissociation of N_2 , in agreement with initial results for TCC.⁶⁹ The CASiTCCSD curves for $n = 2$ and $n = 3$ are qualitatively correct, but exhibit a substantial error at the dissociation limit. We ascribe these shortcomings to two main sources of error: (i) CASiCC is not a genuine multireference method; as a multireference-driven single-reference method, there is a persistent asymmetry in the excitations due to the preference of the reference determinant in the case of near or exact degeneracies. (ii) Additionally, correlation in the external space increases as well upon dissociation so that higher cluster amplitudes must be included to account for this correlation. Hence, the integration of higher-order cluster

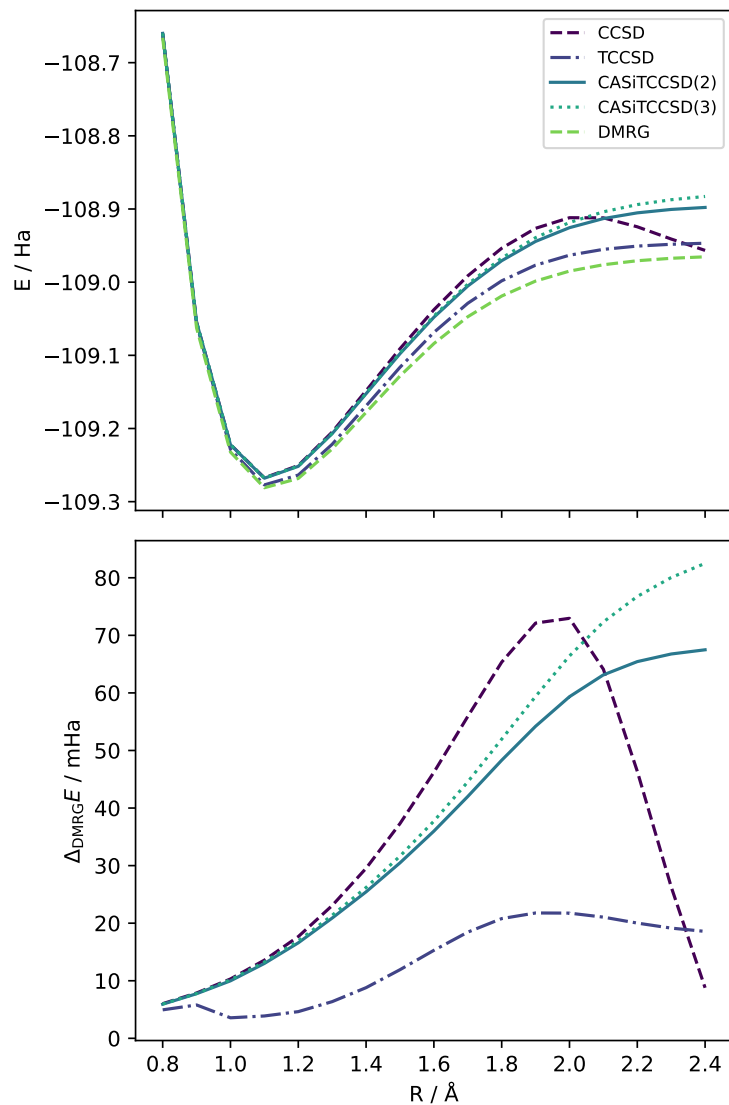


Figure 6: Total electronic energy (top) and energy error with respect to DMRG($m = 2000$) (bottom) for the dissociation of N_2 in Hartree. Shown are results for TCCSD and for CASiTCCSD for different truncation schemes of the BCH expansion. The cc-pVDZ basis set was chosen, which yielded 28 orbitals. For the DMRG reference calculation, all 28 orbitals were all taken into account in order to obtain an energy close to the exact FCI reference. All other results were obtained in a limited orbital space of CAS(6,6).

amplitudes in the external space becomes a critical consideration for the future development of the CASiTCCSD method. Note again that CASiTCCSD(3) and CASieCCSD(3) yielded virtually the same result, however, ecCCSD converged significantly slower in the strong correlation limit.

4.2.2 Dissociation of H₂O

Finally, we examine the symmetric double dissociation of the H₂O molecule with a bond angle of 104.5° and a CAS(6,5). The dissociation curves for CCSD, TCCSD, ecCCSD, CASiTCCSD(3), and DMRG, along with the energy errors of the CC methods relative to DMRG, are provided in Fig. 7. H₂O also becomes strongly correlated in the dissociation limit, which leads again to unphysical results of CCSD. TCCSD, by contrast, correctly dissociates H₂O with an error in the dissociation limit of roughly 10 milliHartree. ecCCSD describes the dissociation qualitatively well, but it is affected by a large error of around 50 milliHartree which has already been discussed in the literature.⁷⁴ CASiTCCSD(3) also cures the deficiencies of CCSD and correctly dissociates the molecule, with an error of around 35 milliHartree, which is in between TCCSD and ecCCSD.

Hence, again we find that CASiTCCSD(3) delivers a systematic improvement over CCSD results. Nonetheless, for H₂O and N₂ TCCSD shows a higher accuracy in the limit of strong correlation. It was also observed recently¹¹³ that, due to error compensation, single-reference TCC yields results similar to the more rigorous Hilbert-space multireference TCC approach even for very strongly correlated systems, also pointing to an error compensation mechanism. The error of CASiCC in the strong correlation regime can be ascribed to the missing correlation in the external space, and to the bias of the reference determinant.

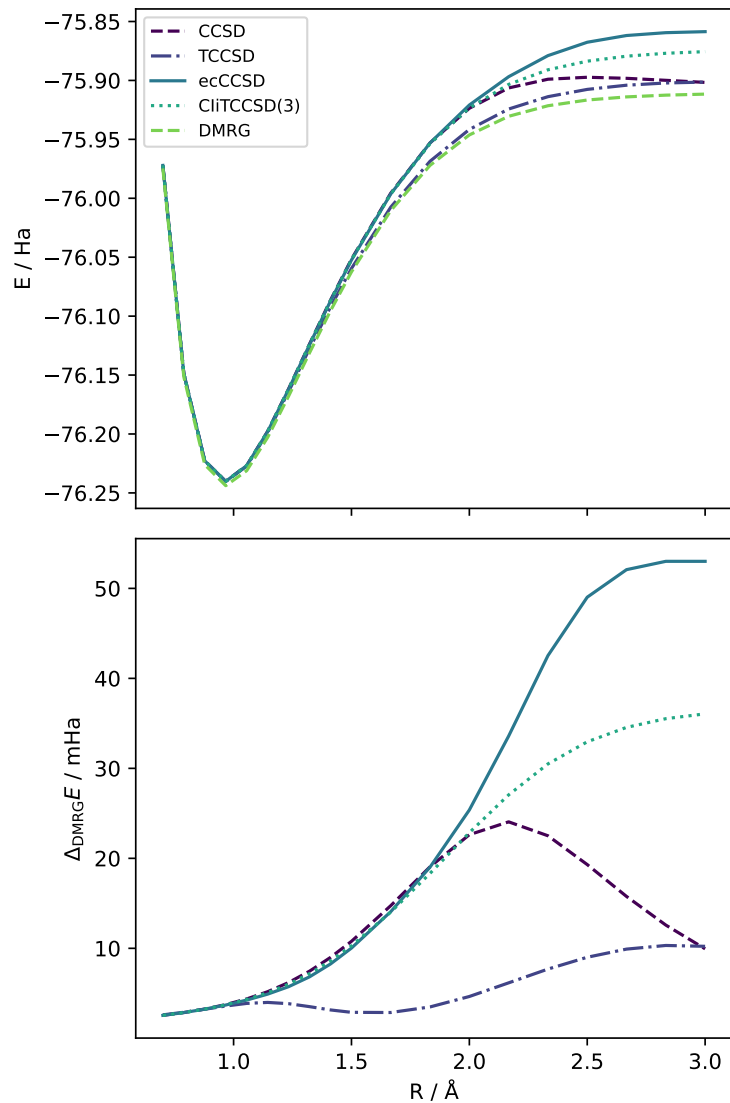


Figure 7: Total electronic energy and energy error with respect to DMRG($m = 2000$) for the dissociation of H_2O in Hartree. Shown are results of CCSD, TCCSD, ecCCSD, and CASiTCCSD(3) calculations. We chose the cc-pVDZ basis set which gives 24 orbitals. For the DMRG calculation, these were all taken into account. Hence, the DMRG results are expected to be very close to the FCI result. By contrast, all other results were obtained in a limited orbital space of CAS(6,5).

5 Conclusions

In this study, we have introduced a configuration interaction approach with iterative coupled cluster feedback (CASiCC). CASiCC iteratively combines complete active space configuration interaction self-consistently with multireference-driven coupled cluster methods. The iterative feedback loop is achieved by similarity transforming the Hamiltonian of the CASCI calculation with the external amplitudes. The similarity transformation results in a nonhermitian Hamiltonian with up to n -body terms. The nonhermiticity does not pose any technical problem, because available CI programs can be easily adapted, and we have demonstrated that the expansion of the Hamiltonian converges already at the third order. Moreover, we showed that the results of CASiCC are quantitatively indistinguishable for the optimization of the amplitudes with tailored coupled cluster from externally corrected coupled cluster. This fact strongly favors the CASiTCC variant, since its implementation and computational scaling are more advantageous, with CASiTCCSD(3) as the most promising candidate.

We studied CASiCC for dissociation curves of H_4 , H_8 , N_2 , and H_2O . Notably, during dissociation of N_2 and H_2O , we observed that TCCSD exhibits superior performance, which may be attributed to the fortunate error cancellation. For further refinement of the CASiCC method, the effect of higher excitations in the external space should be investigated. However, given the fact that we could not systematically improve the TCCSD method iteratively suggests that the accuracy of multireference driven CC methods is inherently limited by the reference bias.

To maintain the cost efficiency similar to that of the standard CCSD method, we are exploring the integration of the DMRG algorithm as a CASCI solver. This approach will be built on our recent work,^{114,115} where we have employed DMRG to evaluate ground state energies of nonhermitian Hamiltonians with up to three-body operators.

Acknowledgments

M. R. gratefully acknowledge financial support by the Swiss National Science Foundation (grant no. 200021_219616), by ETH Zurich (through ETH grant ETH-43 20-2), and by the ‘Quantum for Life Center’ funded by the Novo Nordisk Foundation (grant NNF20OC0059939).

R. F. is grateful for a PhD fellowship awarded by the Günthard Foundation. J. L. and M. L. acknowledge the support from the European Partnership on Metrology (project number 22IEM04 MQB-Pascal), co-financed from the European Union’s Horizon Europe Research and Innovation Programme and by the Participating States.

References

- (1) Helgaker, T.; Jorgensen, P.; Olsen, J. *Molecular electronic-structure theory*; John Wiley & Sons: Chichester, England, 2000.
- (2) Shavitt, I.; Bartlett, R. J. *Many-Body Methods in Chemistry and Physics: MBPT and Coupled-Cluster Theory*; Cambridge Molecular Science; Cambridge University Press, 2009.
- (3) Roos, B. O., et al. The complete active space self-consistent field method and its applications in electronic structure calculations. *Adv. Chem. Phys.* **2007**, *69*, 399–445.
- (4) Ruedenberg, K.; Schmidt, M. W.; Gilbert, M. M.; Elbert, S. Are atoms intrinsic to molecular electronic wavefunctions? I. The FORS model. *Chem. Phys.* **1982**, *71*, 41–49.
- (5) Roos, B. O.; Taylor, P. R.; Sigbahn, P. E. A complete active space SCF method (CASSCF) using a density matrix formulated super-CI approach. *Chem. Phys.* **1980**, *48*, 157–173.
- (6) Huron, B.; Malrieu, J.; Rancurel, P. Iterative perturbation calculations of ground and

- excited state energies from multiconfigurational zeroth-order wavefunctions. *J. Chem. Phys.* **1973**, *58*, 5745–5759.
- (7) Evangelisti, S.; Daudey, J.-P.; Malrieu, J.-P. Convergence of an improved CIPSI algorithm. *Chem. Phys.* **1983**, *75*, 91–102.
- (8) Holmes, A. A.; Tubman, N. M.; Umrigar, C. Heat-bath configuration interaction: An efficient selected configuration interaction algorithm inspired by heat-bath sampling. *J. Chem. Theory Comput.* **2016**, *12*, 3674–3680.
- (9) Smith, J. E.; Mussard, B.; Holmes, A. A.; Sharma, S. Cheap and near exact CASSCF with large active spaces. *J. Chem. Theory Comput.* **2017**, *13*, 5468–5478.
- (10) White, S. R. Density matrix formulation for quantum renormalization groups. *Phys. Rev. Lett.* **1992**, *69*, 2863–2866.
- (11) White, S. R. Density-matrix algorithms for quantum renormalization groups. *Phys. Rev. B* **1993**, *48*, 10345.
- (12) Chan, G. K.-L.; Dorando, J. J.; Ghosh, D.; Hachmann, J.; Neuscamman, E.; Wang, H.; Yanai, T. *Frontiers in Quantum Systems in Chemistry and Physics*; Springer-Verlag, 2008; pp 49–65.
- (13) Chan, G. K.-L.; Zgid, D. The Density Matrix Renormalization Group in Quantum Chemistry. *Annu. Rep. Comput. Chem.* **2009**, *5*, 149–162.
- (14) Marti, K. H.; Reiher, M. The density matrix renormalization group algorithm in quantum chemistry. *Z. Phys. Chem.* **2010**, *224*, 583–599.
- (15) Schollwöck, U. The density-matrix renormalization group in the age of matrix product states. *Ann. Phys.* **2011**, *326*, 96–192.
- (16) Chan, G. K.-L.; Sharma, S. The density matrix renormalization group in quantum chemistry. *Annu. Rev. Phys. Chem.* **2011**, *62*, 465–481.

- (17) Wouters, S.; Van Neck, D. The density matrix renormalization group for ab initio quantum chemistry. *Eur. Phys. J. D* **2014**, *68*, 1–20.
- (18) Kurashige, Y. Multireference electron correlation methods with density matrix renormalisation group reference functions. *Mol. Phys.* **2014**, *112*, 1485–1494.
- (19) Olivares-Amaya, R.; Hu, W.; Nakatani, N.; Sharma, S.; Yang, J.; Chan, G. K.-L. The ab-initio density matrix renormalization group in practice. *J. Chem. Phys.* **2015**, *142*, 34102.
- (20) Szalay, S.; Pfeiffer, M.; Murg, V.; Barcza, G.; Verstraete, F.; Schneider, R.; Legeza, Ö. Tensor product methods and entanglement optimization for ab initio quantum chemistry. *Int. J. Quantum Chem.* **2015**, *115*, 1342–1391.
- (21) Yanai, T.; Kurashige, Y.; Mizukami, W.; Chalupský, J.; Lan, T. N.; Saitow, M. Density matrix renormalization group for ab initio calculations and associated dynamic correlation methods: A review of theory and applications. *Int. J. Quantum Chem.* **2015**, *115*, 283–299.
- (22) Baiardi, A.; Reiher, M. The density matrix renormalization group in chemistry and molecular physics: Recent developments and new challenges. *J. Chem. Phys.* **2020**, *152*, 040903.
- (23) Booth, G. H.; Thom, A. J.; Alavi, A. Fermion Monte Carlo without fixed nodes: A game of life, death, and annihilation in Slater determinant space. *J. Chem. Phys.* **2009**, *131*, 054106.
- (24) Cleland, D.; Booth, G. H.; Alavi, A. A study of electron affinities using the initiator approach to full configuration interaction quantum Monte Carlo. *J. Chem. Phys.* **2011**, *134*, 024112.

- (25) Eriksen, J. J.; Lipparini, F.; Gauss, J. Virtual orbital many-body expansions: A possible route towards the full configuration interaction limit. *J. Phys. Chem. Lett.* **2017**, *8*, 4633–4639.
- (26) Eriksen, J. J.; Anderson, T. A.; Deustua, J. E.; Ghanem, K.; Hait, D.; Hoffmann, M. R.; Lee, S.; Levine, D. S.; Magoulas, I.; Shen, J., et al. The ground state electronic energy of benzene. *J. Phys. Chem. Lett.* **2020**, *11*, 8922–8929.
- (27) Lindh, R.; Galván, I. F. *Quantum Chemistry and Dynamics of Excited States*; John Wiley & Sons, Ltd, 2020; Chapter 10, pp 299–353.
- (28) Andersson, K.; Malmqvist, P.-Å.; Roos, B. O. Second-order perturbation theory with a complete active space self-consistent field reference function. *J. Chem. Phys.* **1992**, *96*, 1218–1226.
- (29) Angeli, C.; Cimiraglia, R.; Evangelisti, S.; Leininger, T.; Malrieu, J.-P. Introduction of n-electron valence states for multireference perturbation theory. *J. Chem. Phys.* **2001**, *114*, 10252–10264.
- (30) Sarkar, R.; Loos, P.-F.; Boggio-Pasqua, M.; Jacquemin, D. Assessing the Performances of CASPT2 and NEVPT2 for Vertical Excitation Energies. *J. Chem. Theory Comput.* **2022**, *18*, 2418–2436.
- (31) Boggio-Pasqua, M.; Jacquemin, D.; Loos, P.-F. Benchmarking CASPT3 vertical excitation energies. *J. Chem. Phys.* **2022**, *157*, 014103.
- (32) Buenker, R. J.; Peyerimhoff, S. D. Individualized configuration selection in CI calculations with subsequent energy extrapolation. *Theor. Chim. Acta* **1974**, *35*, 33–58.
- (33) Meyer, W. In *Methods of Electronic Structure Theory*; Schaefer, H. F., Ed.; Springer US: Boston, MA, 1977; pp 413–446.

- (34) Shavitt, I. In *Methods of Electronic Structure Theory*; Schaefer, H. F., Ed.; Springer US: Boston, MA, 1977; pp 189–275.
- (35) Siegbahn, P. E. Direct configuration interaction with a reference state composed of many reference configurations. *Int. J. Quantum Chem.* **1980**, *18*, 1229–1242.
- (36) Werner, H.-J.; Reinsch, E.-A. The self-consistent electron pairs method for multiconfiguration reference state functions. *J. Chem. Phys.* **1982**, *76*, 3144–3156.
- (37) Buenker, R. J.; Peyerimhoff, S. D. AB Initio Calculations Close to the Full CI Level of Accuracy and their Use for the Interpretation of Molecular Spectra. *New Horizons of Quantum Chemistry*. Dordrecht, 1983; pp 183–219.
- (38) Werner, H.-J.; Knowles, P. J. An efficient internally contracted multiconfiguration–reference configuration interaction method. *J. Chem. Phys.* **1988**, *89*, 5803–5814.
- (39) Shavitt, I. The history and evolution of configuration interaction. *Mol. Phys.* **1998**, *94*, 3–17.
- (40) Shamasundar, K.; Knizia, G.; Werner, H.-J. A new internally contracted multi-reference configuration interaction method. *J. Chem. Phys.* **2011**, *135*, 054101.
- (41) Szalay, P. G.; Muller, T.; Gidofalvi, G.; Lischka, H.; Shepard, R. Multiconfiguration self-consistent field and multireference configuration interaction methods and applications. *Chem. Rev.* **2012**, *112*, 108–181.
- (42) Lischka, H.; Nachtigallova, D.; Aquino, A. J.; Szalay, P. G.; Plasser, F.; Machado, F. B.; Barbatti, M. Multireference approaches for excited states of molecules. *Chem. Rev.* **2018**, *118*, 7293–7361.
- (43) Raghavachari, K.; Trucks, G. W.; Pople, J. A.; Head-Gordon, M. A fifth-order perturbation comparison of electron correlation theories. *Chem. Phys. Lett.* **1989**, *157*, 479–483.

- (44) Bartlett, R. J.; Watts, J.; Kucharski, S.; Noga, J. Non-iterative fifth-order triple and quadruple excitation energy corrections in correlated methods. *Chem. Phys. Lett.* **1990**, *165*, 513–522.
- (45) Jeziorski, B.; Monkhorst, H. J. Coupled-cluster method for multideterminantal reference states. *Phys. Rev. A* **1981**, *24*, 1668.
- (46) Banerjee, A.; Simons, J. The coupled-cluster method with a multiconfiguration reference state. *Int. J. Quantum Chem.* **1981**, *19*, 207–216.
- (47) Mukherjee, D.; Moitra, R. K.; Mukhopadhyay, A. Correlation problem in open-shell atoms and molecules: A non-perturbative linked cluster formulation. *Mol. Phys.* **1975**, *30*, 1861–1888.
- (48) Mukherjee, D. Normal ordering and a Wick-like reduction theorem for fermions with respect to a multi-determinantal reference state. *Chem. Phys. Lett.* **1997**, *274*, 561–566.
- (49) Kutzelnigg, W.; Mukherjee, D. Normal order and extended Wick theorem for a multiconfiguration reference wave function. *J. Chem. Phys.* **1997**, *107*, 432–449.
- (50) Mášik, J.; Hubač, I.; Mach, P. Single-root multireference Brillouin-Wigner coupled-cluster theory: Applicability to the F₂ molecule. *J. Chem. Phys.* **1998**, *108*, 6571–6579.
- (51) Piecuch, P.; Paldus, J. Orthogonally spin-adapted multi-reference Hilbert space coupled-cluster formalism: Diagrammatic formulation. *Theor. Chim. Acta* **1992**, *83*, 69–103.
- (52) Meller, J.; Malrieu, J.; Caballol, R. State-specific coupled cluster-type dressing of multireference singles and doubles configuration interaction matrix. *J. Chem. Phys.* **1996**, *104*, 4068–4076.
- (53) Mahapatra, U. S.; Datta, B.; Bandyopadhyay, B.; Mukherjee, D. State-specific multi-reference coupled cluster formulations: Two paradigms. *Adv. Quantum Chem.* **1998**, *30*, 163–193.

- (54) Mahapatra, U. S.; Datta, B.; Mukherjee, D. A state-specific multi-reference coupled cluster formalism with molecular applications. *Mol. Phys.* **1998**, *94*, 157–171.
- (55) Mahapatra, U. S.; Datta, B.; Mukherjee, D. A size-consistent state-specific multireference coupled cluster theory: Formal developments and molecular applications. *J. Chem. Phys.* **1999**, *110*, 6171–6188.
- (56) Hanrath, M. An exponential multireference wave-function Ansatz. *J. Chem. Phys.* **2005**, *123*, 084102.
- (57) Hanrath, M. Initial applications of an exponential multi-reference wavefunction ansatz. *Chem. Phys. Lett.* **2006**, *420*, 426–431.
- (58) Mahapatra, U. S.; Chattopadhyay, S. Potential energy surface studies via a single root multireference coupled cluster theory. *J. Chem. Phys.* **2010**, *133*, 074102.
- (59) Maitra, R.; Sinha, D.; Mukherjee, D. Unitary group adapted state-specific multi-reference coupled cluster theory: Formulation and pilot numerical applications. *J. Chem. Phys.* **2012**, *137*, 024105.
- (60) Lyakh, D. I.; Musiał, M.; Lotrich, V. F.; Bartlett, R. J. Multireference nature of chemistry: The coupled-cluster view. *Chem. Rev.* **2012**, *112*, 182–243.
- (61) Evangelista, F. A. Perspective: Multireference coupled cluster theories of dynamical electron correlation. *J. Chem. Phys.* **2018**, *149*, 030901.
- (62) Oliphant, N.; Adamowicz, L. The implementation of the multireference coupled-cluster method based on the single-reference formalism. *J. Chem. Phys.* **1992**, *96*, 3739–3744.
- (63) Li, X.; Peris, G.; Planelles, J.; Rajadall, F.; Paldus, J. Externally corrected singles and doubles coupled cluster methods for open-shell systems. *J. Chem. Phys.* **1997**, *107*, 90–98.

- (64) Peris, G.; Rajadell, F.; Li, X.; Planelles, J.; Paldus, J. Externally corrected singles and doubles coupled cluster methods for open-shell systems. II. Applications to the low lying doublet states of OH, NH₂, CH₃ and CN radicals. *Mol. Phys.* **1998**, *94*, 235–248.
- (65) Planelles, J.; Paldus, J.; Li, X. Valence bond corrected single reference coupled cluster approach: III. Simple model of bond breaking or formation. *Theor. Chim. Acta* **1994**, *89*, 59–76.
- (66) Paldus, J.; Planelles, J. Valence bond corrected single reference coupled cluster approach: I. General formalism. *Theor. Chim. Acta* **1994**, *89*, 13–31.
- (67) Peris, G.; Planelles, J.; Paldus, J. Single-reference CCSD approach employing three- and four-body CAS SCF corrections: A preliminary study of a simple model. *Int. J. Quantum Chem.* **1997**, *62*, 137–151.
- (68) Stolarczyk, L. Z. Complete active space coupled-cluster method. Extension of single-reference coupled-cluster method using the CASSCF wavefunction. *Chem. Phys. Lett.* **1994**, *217*, 1–6.
- (69) Kinoshita, T.; Hino, O.; Bartlett, R. J. Coupled-cluster method tailored by configuration interaction. *J. Chem. Phys.* **2005**, *123*, 074106.
- (70) Paldus, J.; Boyle, M. Cluster analysis of the full configuration interaction wave functions of cyclic polyene models. *Int. J. Quantum Chem.* **1982**, *22*, 1281–1305.
- (71) Peris, G.; Planelles, J.; Paldus, J. Single-reference CCSD approach employing three- and four-body CAS SCF corrections: A preliminary study of a simple model. *Int. J. Quantum Chem.* **1997**, *62*, 137–151.
- (72) Deustua, J. E.; Magoulas, I.; Shen, J.; Piecuch, P. Communication: Approaching exact quantum chemistry by cluster analysis of full configuration interaction quantum Monte Carlo wave functions. *J. Chem. Phys.* **2018**, *149*, 151101.

- (73) Magoulas, I.; Gururangan, K.; Piecuch, P.; Deustua, J. E.; Shen, J. Is externally corrected coupled cluster always better than the underlying truncated configuration interaction? *J. Chem. Theory Comput.* **2021**, *17*, 4006–4027.
- (74) Lee, S.; Zhai, H.; Sharma, S.; Umrigar, C. J.; Chan, G. K.-L. Externally corrected ccSD with renormalized perturbative triples (R-ecCCSD(T)) and the density matrix renormalization group and selected configuration interaction external sources. *J. Chem. Theory Comput.* **2021**, *17*, 3414–3425.
- (75) Faulstich, F. M.; Máté, M.; Laestadius, A.; Csirik, M. A.; Veis, L.; Antalík, A.; Brabec, J.; Schneider, R.; Pittner, J.; Kvaal, S., et al. Numerical and theoretical aspects of the DMRG-TCC method exemplified by the nitrogen dimer. *J. Chem. Theory Comput.* **2019**, *15*, 2206–2220.
- (76) Faulstich, F. M.; Laestadius, A.; Legeza, O.; Schneider, R.; Kvaal, S. Analysis of the tailored coupled-cluster method in quantum chemistry. *SIAM J. Numer. Anal.* **2019**, *57*, 2579–2607.
- (77) Mörchen, M.; Freitag, L.; Reiher, M. Tailored coupled cluster theory in varying correlation regimes. *J. Chem. Phys.* **2020**, *153*, 244113.
- (78) Primas, H. Generalized perturbation theory in operator form. *Rev. Mod. Phys.* **1963**, *35*, 710.
- (79) Głazek, S. D.; Wilson, K. G. Renormalization of hamiltonians. *Phys. Rev. D* **1993**, *48*, 5863.
- (80) Wegner, F. Flow-equations for Hamiltonians. *Ann. Phys. (Leipzig)* **1994**, *506*, 77–91.
- (81) White, S. R. Numerical canonical transformation approach to quantum many-body problems. *J. Chem. Phys.* **2002**, *117*, 7472–7482.

- (82) Tsukiyama, K.; Bogner, S.; Schwenk, A. In-medium similarity renormalization group for nuclei. *Phys. Rev. Lett.* **2011**, *106*, 222502.
- (83) Tsukiyama, K.; Bogner, S.; Schwenk, A. In-medium similarity renormalization group for open-shell nuclei. *Phys. Rev. C* **2012**, *85*, 061304.
- (84) Hergert, H.; Bogner, S.; Morris, T.; Schwenk, A.; Tsukiyama, K. The in-medium similarity renormalization group: A novel ab initio method for nuclei. *Phys. Rep.* **2016**, *621*, 165–222.
- (85) Hergert, H. In-medium similarity renormalization group for closed and open-shell nuclei. *Phys. Scr.* **2016**, *92*, 023002.
- (86) Gebrerufael, E.; Vobig, K.; Hergert, H.; Roth, R. Ab initio description of open-shell nuclei: merging no-core shell model and in-medium similarity renormalization group. *Phys. Rev. Lett.* **2017**, *118*, 152503.
- (87) Tichai, A.; Knecht, S.; Kruppa, A. T.; Legeza, Ö.; Moca, C. P.; Schwenk, A.; Werner, M. A.; Zarand, G. Combining the in-medium similarity renormalization group with the density matrix renormalization group: Shell structure and information entropy. *Phys. Lett. B* **2023**, *845*, 138139.
- (88) Evangelista, F. A. A driven similarity renormalization group approach to quantum many-body problems. *J. Chem. Phys.* **2014**, *141*, 054109.
- (89) Li, C.; Evangelista, F. A. Multireference theories of electron correlation based on the driven similarity renormalization group. *Annu. Rev. Phys. Chem.* **2019**, *70*, 245–273.
- (90) Li, C.; Evangelista, F. A. Multireference driven similarity renormalization group: A second-order perturbative analysis. *J. Chem. Theory Comput.* **2015**, *11*, 2097–2108.
- (91) Li, C.; Evangelista, F. A. Driven similarity renormalization group: Third-order multireference perturbation theory. *J. Chem. Phys.* **2017**, *146*, 124132.

- (92) Kowalski, K. Properties of coupled-cluster equations originating in excitation sub-algebras. *J. Chem. Phys.* **2018**, *148*, 094104.
- (93) Bauman, N. P.; Bylaska, E. J.; Krishnamoorthy, S.; Low, G. H.; Wiebe, N.; Granade, C. E.; Roetteler, M.; Troyer, M.; Kowalski, K. Downfolding of many-body Hamiltonians using active-space models: Extension of the sub-system embedding sub-algebras approach to unitary coupled cluster formalisms. *J. Chem. Phys.* **2019**, *151*, 014107.
- (94) Bauman, N. P.; Kowalski, K. Coupled cluster downfolding methods: The effect of double commutator terms on the accuracy of ground-state energies. *J. Chem. Phys.* **2022**, *156*, 094106.
- (95) Kowalski, K. Sub-system self-consistency in coupled cluster theory. *J. Chem. Phys.* **2023**, *158*, 054101.
- (96) Li, C.; Evangelista, F. A. Towards numerically robust multireference theories: The driven similarity renormalization group truncated to one-and two-body operators. *J. Chem. Phys.* **2016**, *144*, 164114.
- (97) Li, C.; Evangelista, F. A. Connected three-body terms in single-reference unitary many-body theories: Iterative and perturbative approximations. *The Journal of Chemical Physics* **2020**, *152*, 234116.
- (98) Chan, G. K.; Van Voorhis, T. Density-matrix renormalization-group algorithms with nonorthogonal orbitals and non-Hermitian operators, and applications to polyenes. *J. Chem. Phys.* **2005**, *122*, 204101.
- (99) Kvaal, S. Three Lagrangians for the complete-active space coupled-cluster method. *arXiv preprint [arXiv:2205.08792](https://arxiv.org/abs/2205.08792)* **2022**,

- (100) Monkhorst, H. J. Calculation of properties with the coupled-cluster method. *Int. J. Quantum Chem.* **1977**, *12*, 421–432.
- (101) Paldus, J.; Li, X. A critical assessment of coupled cluster method in quantum chemistry. *Adv. Chem. Phys.* **1999**, *110*, 1–175.
- (102) Evangelista, F. A. Automatic derivation of many-body theories based on general Fermi vacua. *J. Chem. Phys.* **2022**, *157*, 064111.
- (103) Jakob, W.; Rhineland, J.; Moldovan, D. pybind11 — Seamless operability between C++11 and Python. 2024; <https://github.com/pybind/pybind11>.
- (104) Mörchen, M.; Feldmann, R.; Reiher, M. CASiCC Package 1.0.0. 2024; <https://doi.org/10.5281/zenodo.10927298>.
- (105) Keller, S.; Dolfi, M.; Troyer, M.; Reiher, M. An efficient matrix product operator representation of the quantum chemical Hamiltonian. *J. Chem. Phys.* **2015**, *143*, 244118.
- (106) Legeza, Ö.; Sólyom, J. Optimizing the density-matrix renormalization group method using quantum information entropy. *Phys. Rev. B* **2003**, *68*, 195116.
- (107) Barcza, G.; Legeza, Ö.; Marti, K. H.; Reiher, M. Quantum-information analysis of electronic states of different molecular structures. *Phys. Rev. A* **2011**, *83*, 012508.
- (108) Chan, G. K.-L.; Kállay, M.; Gauss, J. State-of-the-art density matrix renormalization group and coupled cluster theory studies of the nitrogen binding curve. *J. Chem. Phys.* **2004**, *121*, 6110–6116.
- (109) Binkley, J. S.; Pople, J. A.; Hehre, W. J. Self-consistent molecular orbital methods. 21. Small split-valence basis sets for first-row elements. *J. Am. Chem. Soc.* **1980**, *102*, 939–947.

- (110) Dunning Jr., T. H. Gaussian basis sets for use in correlated molecular calculations. I. The atoms boron through neon and hydrogen. *J. Chem. Phys.* **1989**, *90*, 1007–1023.
- (111) Sun, Q.; Berkelbach, T. C.; Blunt, N. S.; Booth, G. H.; Guo, S.; Li, Z.; Liu, J.; McClain, J. D.; Sayfutyarova, E. R.; Sharma, S., et al. PySCF: the Python-based simulations of chemistry framework. *Wiley Interdiscip. Rev. Comput. Mol. Sci.* **2018**, *8*, e1340.
- (112) Sun, Q.; Zhang, X.; Banerjee, S.; Bao, P.; Barbry, M.; Blunt, N. S.; Bogdanov, N. A.; Booth, G. H.; Chen, J.; Cui, Z.-H., et al. Recent developments in the PySCF program package. *J. Chem. Phys.* **2020**, *153*, 024109.
- (113) Demel, O.; Brandejs, J.; Lang, J.; Brabec, J.; Veis, L.; Legeza, O.; Pittner, J. Hilbert space multireference coupled cluster tailored by matrix product states. *J. Chem. Phys.* **2023**, *159*, 224115.
- (114) Baiardi, A.; Reiher, M. Transcorrelated density matrix renormalization group. *J. Chem. Phys.* **2020**, *153*, 164115.
- (115) Baiardi, A.; Lesiuk, M.; Reiher, M. Explicitly correlated electronic structure calculations with transcorrelated matrix product operators. *J. Chem. Theory Comput.* **2022**, *18*, 4203–4217.